Wetlands
DOI 10.1007/s13157-016-0744-9

ORIGINAL RESEARCH

# Spatial Configuration Trends in Coastal Louisiana from 1985 to 2010

**Brady R. Couvillion[1] · Michelle R. Fischer[1] · Holly J. Beck[1] · William J. Sleavin[2]**

Received: 19 August 2015 / Accepted: 21 January 2016


**Abstract** From 1932 to 2010, coastal Louisiana has experienced a net loss of 4877 km$^2$ of wetlands. As the area of these wetlands has changed, so too has the spatial configuration of the landscape. The resulting landscape is a mosaic of patches of wetlands and open water. This study examined the spatial and temporal variability of trajectories of landscape configuration and the relation of those patterns to the trajectories of land change in wetlands during a 1985–2010 observation period. Spatial configuration was quantified using multi-temporal satellite imagery and an aggregation index (AI). The results of this analysis indicate that coastal Louisiana experienced a reduction in the AI of coastal wetlands of 1.07 %. In general, forested wetland and fresh marsh types displayed the highest aggregation and stability. The remaining marsh types, (intermediate, brackish, and saline) all experienced disaggregation during the time period, with increasing severity of disaggregation along an increasing salinity gradient. Finally, a correlation ($r^2 = 0.5562$) was found between AI and the land change rate for the subsequent period, indicating that fragmentation can increase the vulnerability of wetlands to further wetland loss. These results can help identify coastal areas which are susceptible to future wetland loss.

✉ Brady R. Couvillion
couvillionb@usgs.gov

[1] Wetland and Aquatic Research Center, Coastal Restoration Assessment Branch, c/o Livestock Show Office, U.S. Geological Survey, Parker Coliseum, LSU, Baton Rouge, LA 70803, USA

[2] Cherokee Nation Technologies, Inc., Tulsa, OK, USA

**Keywords** Wetland fragmentation · Wetland configuration · Land change · Wetland loss · Coastal Louisiana · Landscape fragmentation

## Introduction

In coastal Louisiana, many areas that were once vast expanses of contiguous marsh are now comprised of a highly fragmented mosaic of patches (Suir et al. 2013). Other areas have now completely converted to open water. Landscape configuration and connectivity affect fundamental ecosystem processes, which determine the trajectories of ecological condition (O'Neill et al. 1997; Kupfer 2012). Habitat quality is not determined solely by the quantity of habitat, but also by its configuration in the landscape (Kelly et al. 2011). Additionally, most conceptual models of wetland loss in Louisiana suggest that fragmented marsh will eventually convert to open water without any restoration efforts (Peyronnin et al. 2013). Turner and Rao (1990) noted that "it is clear that wetland breakup, not erosion at the pond-lake edge, is the dominant form of wetland-to-open water conversion." The process of fragmentation of a continuous habitat begins with a reduction in habitat area and an increase in edge. The remaining habitat may initially maintain substantial connectivity but will become increasingly fragmented as habitat loss continues (Jaeger 2000; Neel et al. 2004). Therefore, the quantification of landscape configuration and its change is an important precursor to an understanding of the effects of that change (Tischendorf 2001) and predicting which areas of the coast are more susceptible to loss.

The ability to quantify landscape configuration is an important part of studying landscape function and change because it is believed that the two are inherently related (Kupfer 2012). Studying landscape pattern is therefore

Published online: 13 February 2016

essential to understanding the underlying and resulting ecological processes. Previous studies have focused on the impact of configuration and fragmentation on habitat suitability, dispersal, and other biotic factors (Turner and Rao 1990; Forman 1995; Saura 2004; Suir et al. 2013). Few studies however have focused on fragmentation as a function of, and a contributor to, morphologic change (Yang and Liu 2005). Harris (1988) noted wetlands that have a large perimeter-to-area ratio are particularly susceptible to fragmentation. Yet fundamental questions remain regarding the influence of spatial configuration of wetlands on the susceptibility of those wetlands to further loss.

This study utilized a landscape metric known as the aggregation index (AI) to quantify landscape configuration and assess historical trends through the use of remotely sensed imagery and other geospatial datasets. Previous studies have suggested the specific configuration metric chosen for analysis should reflect the landscape pattern of interest and the processes which relate to that pattern (McGarigal 2002; Neel et al. 2004). While many other types of landscape indices exist, an aggregation metric best suits our goals to better understand the spatial character, arrangement and position of isolated patches within a wetland. This particular index quantifies the tendency of a patch to be spatially aggregated (i.e. occur in large, aggregated distributions) (McGarigal 2002). The aggregation index is class or land cover category specific and provides a quantitative basis to correlate the spatial pattern of a class with a specific process (He et al. 2000). While many other ecological studies aim to better understand the connection between species behavior and landscape structure, our focus relates to the integrity of the wetland landscape.

The repetition of observations, length of record, and spatial coverage available from many types of satellite imagery is useful for long-term monitoring of large expanses of landscapes (O'Neill et al. 1997, Yang and Liu 2005; Suir et al. 2013). While quantifying landscape composition and configuration on a specific date is useful, the real value of remotely sensed imagery is a historical record. In this study, we tracked landscape configuration over a 25 year period from 1985–2010. Trends of configuration change were examined to determine the trajectory of aggregation or disaggregation in coastal Louisiana and to provide information regarding the possible impacts of these trends. The historical configuration trend output was then compared to land area composition trends in periods following the quantification of aggregation to determine the existence and strength of a relationship between the two factors.

Our specific objectives were to: (1) develop an easily implemented method for quantifying wetland configuration across space and time; (2) assess historical trends in wetland configuration from 1985–2010; (3) compare trends of configuration change to those of wetland area change for a possible linkage; (4) discuss the possible implications of configuration change on future rates of wetland loss; and (5) consider the implications of this research on restoration activities.

## Study Area

Coastal Louisiana encompasses an area of about 37,780 km$^2$ of wetlands and open water (Fig. 1). These wetlands are composed of forested wetlands, fresh, intermediate, brackish, and saline marsh. Louisiana's wetlands are generally considered one of the most important environments in the United States, as they support the second largest commercial fishery in the United States (NOAA 2010), contain five of the nation's top 20 ports (Bureau of Transportation Statistics 2013), and 20 % of the nation's oil and gas supply comes from, or is transported

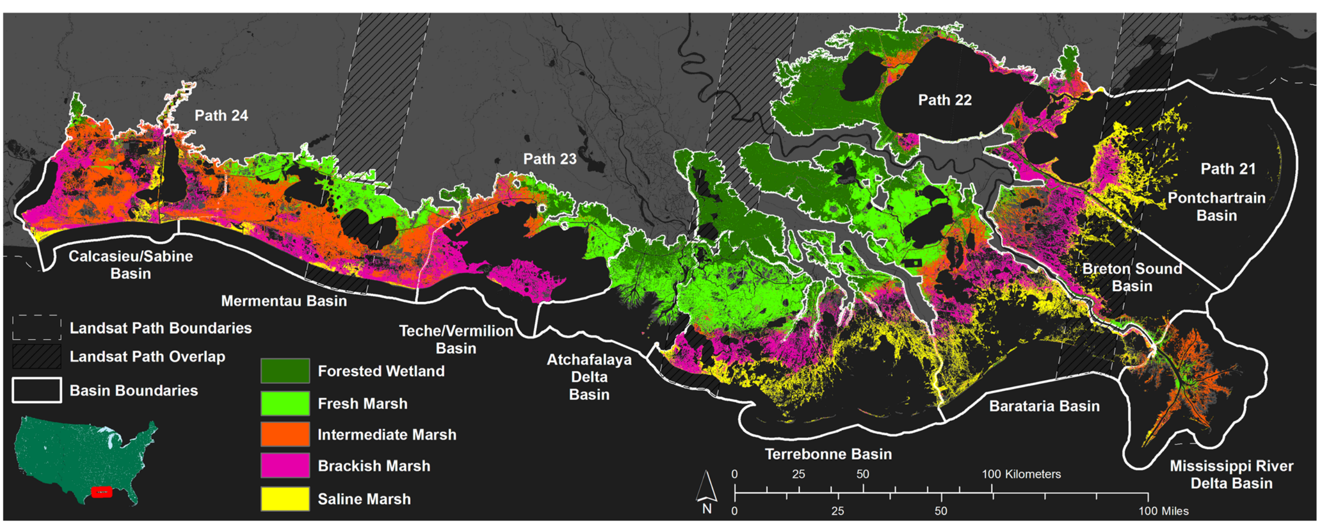


**Fig. 1** Map of the study area in coastal Louisiana which includes Landsat path boundaries, basin boundaries, and 2013 wetland marsh zones (Sasser et al. 2014). The Chenier Plain consists of Calcasieu-Sabine, Mermentau, and Teche-Vermilion hydrologic basins. The Deltaic Plain consists of Atchafalaya, Terrebonne, Barataria, Mississippi River Delta, Breton Sound, and Pontchartrain hydrologic basins

through, these wetlands (LA DNR 2004). However, this coast is also considered to be one of the most at-risk environments in the nation, losing a quarter of these wetlands in the past 78 years (Couvillion et al. 2011).

## Methods

### Imagery

The first step in assessing landscape configuration is characterizing landscape composition. To do so, this analysis used multi-temporal satellite imagery from 1985–2010. The number of dates varied depending upon the path/row (Fig. 1) of the imagery. Imagery consisted of data from Landsat 5 Thematic Mapper (TM) and Landsat 7 Enhanced Thematic Mapper Plus (ETM+) both of which have spatial resolutions of 30 m. Landsat 7 data was only used for the 1999–2003 time period, the only period in which the scan line corrector (SLC) on the satellite was functioning properly. Only cloud-free images were utilized in this study to eliminate the need for cloud recognition algorithms and to remove a possible source of contamination. Imagery used in this analysis is detailed in Table 1.

Satellite images were classified into land/water categories using a methodology which relies heavily on thresholding of the modified Normalized Difference Water Index (mNDWI) (Xu 2006). Index results defined an initial land and water delineation, however unsupervised classification was then used to check the initial datasets for errors. Classes such as floating aquatic vegetation and mudflats which can often be incorrectly classified as land were recoded back to a water category via expert analysis. Land cover types such as forested and herbaceous wetlands which are periodically inundated are still considered land within the classification system. Once the classified land/water datasets for all dates were completed, the aggregation index, our chosen landscape metric, was calculated.

### Accuracy Assessment of Land/Water Classifications

Conducting traditional accuracy assessments of more than 200 images, each containing an average of approximately 80 million pixels for a total of more than 17 billion pixels analyzed in this effort was not feasible. Indeed, determining accuracy at even a 0.1 % sample would require image-interpreter decisions at 17 million locations, requiring approximately 30, 000 hours to complete. Therefore, accuracy of the land/water classifications was assessed within land-cover change groups for a subset of images. Three land-cover change groups were delineated using the variability among all images examined. Group 1 contained only pixels which were consistently

**Table 1** Julian dates of imagery used in this effort by path (WRS-2)

| Path 21 | Path 22 | Path 23 | Path 24 |
|---|---|---|---|
| 1984085; | 1,984,097; | 1,985,026; | 1,984,335; |
| 1,987,114; | 1,985,019; | 1,986,013; | 1,985,337; |
| 1,987,290; | 1,986,086; | 1,986,237; | 1,987,039; |
| 1,987,322; | 1,987,281; | 1,986,301; | 1,987,247; |
| 1987338; | 1,988,028; | 1,987,288; | 1,988,026; |
| 1,988,053; | 1,988,044; | 1,988,115; | 1,988,250; |
| 1,989,295; | 1,990,305; | 1,988,339; | 1,989,284; |
| 1,989,359; | 1,990,321; | 1,989,069; | 1,989,348; |
| 1991269; | 1,991,068; | 1,989,261; | 1,990,287; |
| 1,993,066; | 1,992,279; | 1,989,293; | 1,991,290; |
| 1,993,274; | 1,993,073; | 1,990,328; | 1,991,338; |
| 1,994,021; | 1,994,092; | 1,991,091; | 1,992,293; |
| 1995008; | 1,994,268; | 1,992,014; | 1,993,359; |
| 1,995,024; | 1,995,271; | 1,992,286; | 1,994,090; |
| 1,995,104; | 1,995,319; | 1,992,334; | 1,995,077; |
| 1,995,344; | 1,996,098; | 1,993,064; | 1,995,141; |
| 1996027; | 1,997,036; | 1,993,272; | 1,997,066; |
| 1,996,107; | 1,997,276; | 1,993,304; | 1,997,290; |
| 1,998,048; | 1,998,039; | 1,995,246; | 1,997,306; |
| 1,999,019; | 1,998,055; | 1,995,278; | 1,998,069; |
| 1999259; | 1,999,010; | 1,995,294; | 1,999,024; |
| 1,999,307; | 1,999,026; | 1,995,326; | 1,999,296; |
| 1,999,331; | 1,999,258; | 1,996,009; | 1,999,312; |
| 1,999,363; | 1,999,266; | 1,996,025; | 1,999,320; |
| 2000014; | 1,999,274; | 1,996,121; | 2,000,059; |
| 2,001,064; | 1,999,298; | 1,996,297; | 2,000,331; |
| 2,001,288; | 1,999,322; | 1,996,313; | 2,001,005; |
| 2,001,320; | 1,999,330; | 1,997,011; | 2,001,269; |
| 2001360; | 1,999,362; | 1,997,123; | 2,001,301; |
| 2,002,355; | 2,000,005; | 1,998,062; | 2,002,008; |
| 2,003,006; | 2,000,021; | 1,998,094; | 2,003,323; |
| 2,003,014; | 2,000,037; | 1,998,350; | 2,004,038; |
| 2003078; | 2,000,109; | 1,999,081; | 2,004,070; |
| 2,003,302; | 2,000,261; | 1,999,257; | 2,004,230; |
| 2,003,318; | 2,000,285; | 1,999,265; | 2,004,310; |
| 2,004,049; | 2,000,325; | 1,999,297; | 2,005,280; |
| 2004289; | 2,001,271; | 2,000,116; | 2,005,296; |
| 2,004,353; | 2,001,303; | 2,000,332; | 2,006,043; |
| 2,005,259; | 2,001,335; | 2,000,340; | 2,008,049; |
| 2,005,291; | 2,002,058; | 2,001,270; | 2,008,321; |
| 2006326; | 2,002,362; | 2,001,310; | 2,008,337; |
| 2,007,025; | 2,003,005; | 2,002,081; | 2,009,019; |
| 2,008,076; | 2,003,277; | 2,002,289; | 2,009,035; |
| 2,008,300; | 2,003,293; | 2,002,321; | 2,009,051; |
| 2009030; | 2,005,282; | 2,003,004; | 2,009,291; |
| 2,010,033; | 2,006,301; | 2,003,332; | 2,009,307; |
| 2,010,273; | 2,007,064; | 2,003,364; | 2,010,022 |
| 2,010,289 | 2,007,096; | 2,004,271; | |
| | 2,008,275; | 2,004,287; | |
| | 2,008,307; | 2,005,289; | |
| | 2,009,021; | 2,006,036; | |
| | 2,009,037; | 2,006,100; | |
| | 2,009,293; | 2,006,308; | |
| | 2,010,056; | 2,006,324; | |
| | 2,010,280; | 2,007,263; | |
| | 2,011,043 | 2,008,058; | |
| | | 2,008,106; | |
| | | 2,008,282; | |
| | | 2,008,314; | |
| | | 2,008,330; | |
| | | 2,009,316; | |
| | | 2,010,287 | |

classified as land in all images analyzed and made up approximately 30 % of the study area (11,267 sq.km.). Group 2 contained only pixels which were consistently classified as water in all images analyzed accounting for approximately 51 % of the study area (19,154 sq.km.). The remaining group, group 3, was made up of pixels which contained variability in land/water classification over the study period. This group made up approximately 19 % of the study area (7135 sq.km.).

Accuracy was assessed within each of these groups in two, randomly-selected images per path/row. For each image, a stratified, random sample was taken within each land cover group. A 0.001 % sample was taken in group 1 and group 2, while a 0.01 % sample was taken in group 3. In this way, effort was focused within the group most likely to contain errors, thereby providing more information in the areas of least confidence. Truth was assigned by an image-interpreter at these points, and that truth was then compared to the original classifications to assess accuracy in each group.

### Aggregation Index Tool Methods

To calculate the AI, the number of like contiguous adjacencies between the pixels of the class of interest (land) were first determined. This approach used a maximum of eight adjacencies defined by the four cardinal compass directions as well as the four diagonal adjacencies. In order for pixels at the edge of any given area of interest (AOI) to have a total possible eight adjacencies, adjacencies from pixels immediately outside the AOI were included in the calculations.

For this study, AI was calculated at the landscape (LAI) level. LAI has a range of values from 0–100 and utilizes the percent area occupied by the class within a given AOI to modify the AI value. LAI was calculated using the following equation:

$$LandscapeAI = \sum \frac{AdjacenciesPerPixel}{ClassPixelCount * 8} * PercentAOI * 100$$

where $AdjacenciesPerPixel$ = the number of adjacencies of like class value per pixel, $ClassPixelCount$ = the number of pixels of the class within the AOI, and $PercentAOI$ = the decimal percent area occupied by the class within the AOI.

For this effort, AI had to be calculated over a million times at varying scales, and as such, computational efficiency was a necessity. In order to facilitate the calculation of LAI an automated Geographic Information System (GIS)-based tool was developed. This tool was written using the Python scripting language. The ability to automate the calculation process was an integral part of tool development.

The most highly aggregated and disaggregated forms of the AI are included in Fig. 2. For a given land pixel, the most disaggregated state is represented in Fig. 2a and the most aggregated state is shown in Fig. 2b.

In order to calculate and compare AI values across path/rows, a grid assessment was performed. Land/water datasets were analyzed in each path/row separately, and were then summarized on a coastwide basis using a 250 × 250 m grid. LAI and percent land were summarized per 250 m grid cell for every date of imagery included in each path/row. Because each of the four coastwide path/rows has a different number of images it was necessary to develop a way to unify the AI values across the whole coast. To deal with the disparities in spatial coverage, we calculated weighted moving averages wherein a minimum of three dates of imagery that occupy or surround a single year are weighed and averaged based on their distance from the goal year. Not only does this facilitate coastwide assessments, it also lessens the impact of abnormalities in any one date. For example, abnormally high or low water levels on a single date would be mitigated by the inclusion of multiple dates in any one data point. The end result is a coastwide moving average AI value that represented every year of imagery (1985–2010). This allows us to make comparisons between AI values which occupy different path/rows.

## Results and Discussion

### Accuracy Assessment of Land/Water Classifications

The average accuracies were 94.3 % within the areas of consistent land (group 1), 99.7 % for the areas of consistent water (group 2), and 90.8 % for the areas which varied among land and water categories (group 3). Those accuracies were

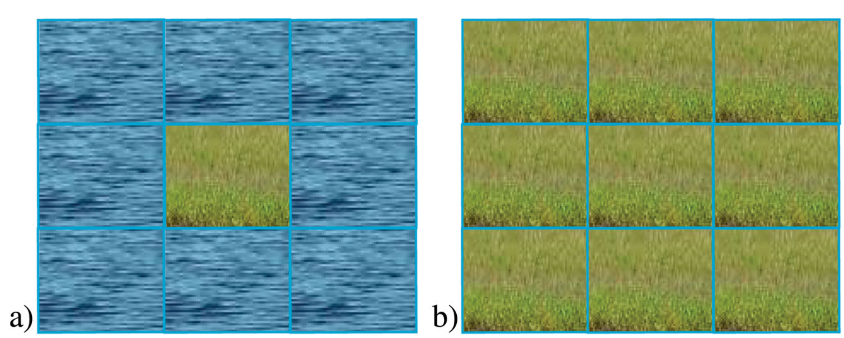


**Fig. 2** Examples of a **a** disaggregated (LAI = 0 %) versus **b** aggregated (LAI = 100 %) landscape. Where blue represents water and green represents land

multiplied by the percentage of the study area within each group, leading to an estimated overall accuracy of 96.4 % when averaged for all images used in this study. Overall accuracy values of this magnitude are generally considered high for remotely-sensed classifications however, the fact that the classifications contain only two categories and the inclusion of areas of persistent land and water in these calculations may explain the high values. The accuracy within group 3 may be the value which is most applicable to the areas of interest in this study however, it is important to remember that areas of stable land are of particular importance to this study also.

In general, these land/water datasets are considered extremely accurate. However, it is important to remember the spatial resolution of the images (30 m) and there may be some features which are too small for the sensor and the image analyst to detect. The accuracy values provided are intended to provide some overall context regarding the general accuracies of the datasets as a whole.

## Spatial Configuration

The results of this analysis indicate that aggregation of coastal Louisiana wetlands varies in time and space. To better understand these patterns we considered AI at the coastwide, basin/marsh type, and restoration site scale.

### Coastwide

In general, forested wetland landscapes tend to be the most aggregated, with AI values averaging 96.61 % (Fig. 3). These landscapes also tend to be the most stable, with no disaggregation observed over the time period, and a slight overall trend toward aggregation (0.00688 %/year). This is consistent with trends of wetland loss which have shown forested wetlands to be very stable landscapes (Barras 2006, 2007). Fresh marsh was the second most aggregated and stable wetland type, with values averaging 72.45 % and a slight trend (0.0229 %/year) toward aggregation observed over the time period.

The remaining marsh types, (intermediate, brackish, and saline) are generally comprised of more fragmented landscapes than that of forested wetlands and fresh marsh. While the general trend is decreasing aggregation with increasing salinity among marsh types, intermediate and brackish marshes often displayed similar aggregation trends. Intermediate marsh coastwide AI values averaged 67.32 % and experienced a trend toward disaggregation by 0.21 %/year, while brackish marsh coastwide AI values averaged 68.86 %, and experienced a trend of disaggregation of 0.277 %/year over the same time period. Trend analysis suggests that although brackish marsh is currently more aggregated on average, it is disaggregating more quickly.

Saline marsh was least aggregated marsh type, with coastwide values averaging 40.31 % and has experienced the greatest trend toward disaggregation at 0.4 %/year over the study period. Saline marshes are generally exposed to more erosion as a result of their position in areas of high wave energy. This erosion has contributed to, and is exacerbated by wetland fragmentation. Additionally, saline marshes often occur in regions of the coast experiencing the highest rates of eustatic sea level rise (ESLR) and subsidence (DeMarco et al.

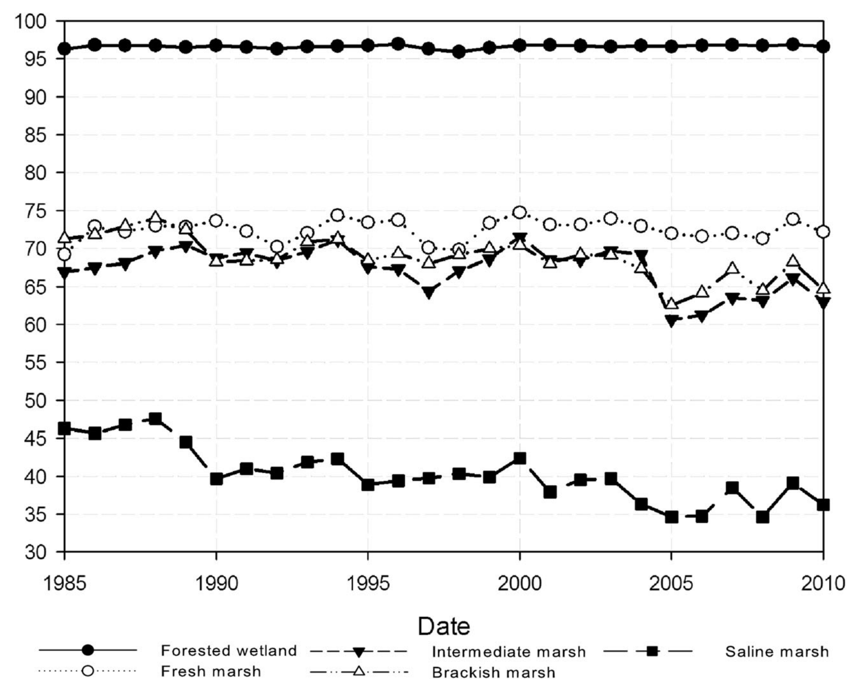


**Fig. 3** Coastwide average landscape aggregation index by marsh type in coastal Louisiana (1985–2010)

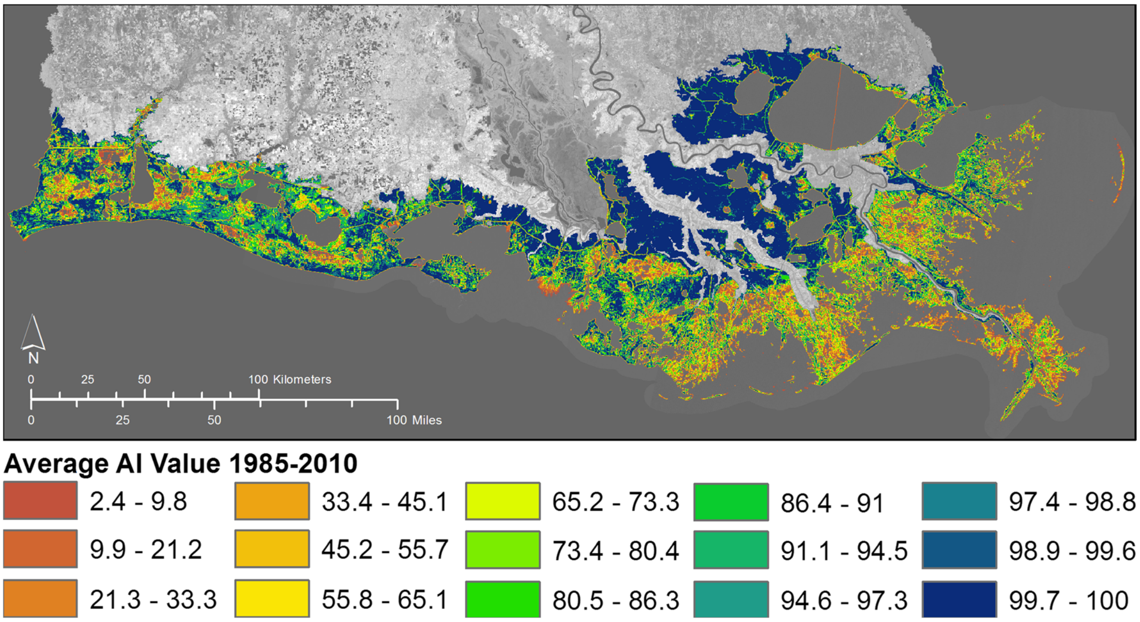


**Fig. 4** Average AI in coastal Louisiana (1985–2010). Lower AI values represent areas in which wetlands are in a more disaggregated state

2012), both of which contribute to the loss and fragmentation of this marsh type.

AI varies spatially across coastal Louisiana (Fig. 4). Some of the most obvious patterns observed in Fig. 4 are the large expanses of wetland area with high AI values in the upper portions of Terrebonne, Barataria, and Pontchartrain basins. These correspond to forested wetland areas that are both contiguous and predominantly stable. Figure 4 also shows a band of low AI values which stretches from lower portions of Terrebonne and Barataria basins and into Breton Sound basin. This band of low AI values corresponds to an area of elevated wetland loss in the Deltaic Plain delineated by white arches in Fig. 5 (Couvillion et al. 2011). Finally, another interesting mosaic of patches exists in the Chenier Plain in southwest coastal Louisiana. This region is heavily managed and the hydrology in the region has been altered, resulting in a patchwork of aggregated and disaggregated landscapes.

Rather than looking at AI on a given date, or an average of dates, looking at overall trends in AI in a spatial context is very informative regarding how the landscape is changing. For this analysis, a simple linear trend was calculated for each 250 m grid cell. The slope of those

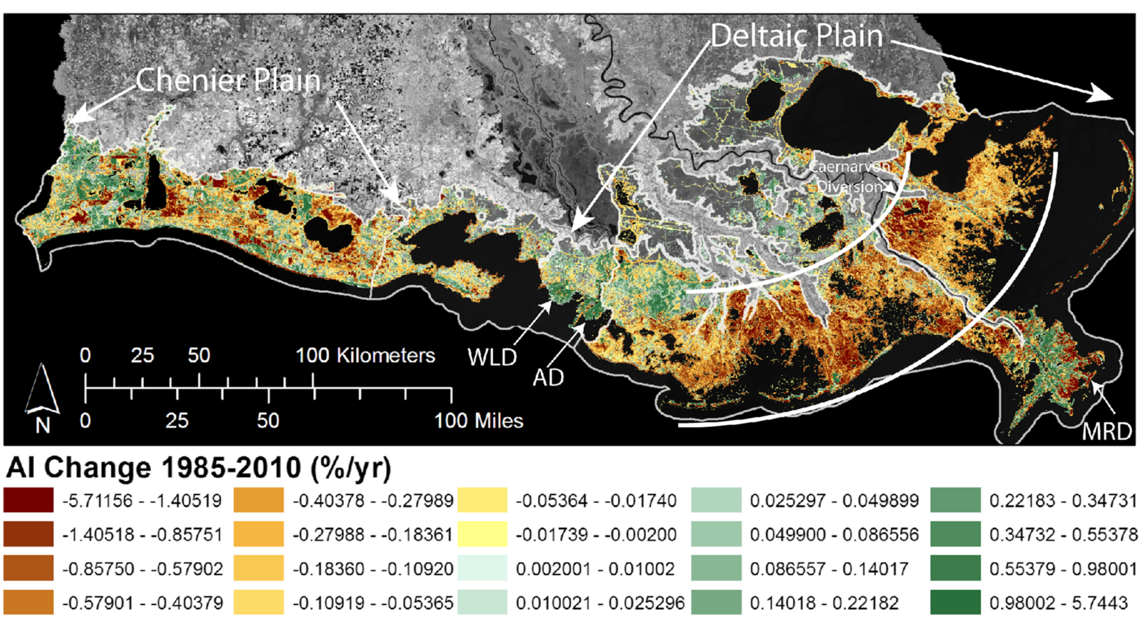


**Fig. 5** Linear change rates of the landscape aggregation index in coastal Louisiana (1985–2010). Wax Lake Delta indicated as WLD. Atchafalaya Delta indicated as AD. Mississippi River Delta indicated as MRD

trends is represented in Fig. 5. Red symbologies in Fig. 5 represent areas experiencing disaggregation, while green symbologies represent aggregation over the time period. Areas of little to no change with regard to aggregation are transparent in this representation. It is evident from Fig. 5 that trends of aggregation and disaggregation vary substantially in space across coastal Louisiana, but disaggregation dominates the landscape. Areas experiencing more rapid disaggregation are shown in darker red symbologies. Many of these areas occur in the same previously mentioned band of elevated wetland loss and disaggregation shown in Fig. 5.

Green symbologies are less prevalent in Fig. 5, however there are specific areas in which clear trends of aggregation are occurring. Actively prograding deltas such as the Wax Lake Delta (WLD), Atchafalaya Delta (AD) and Mississippi River Delta (MRD) are aggregating. Other regions, such as the Chenier Plain, are experiencing less distinct patches of aggregation mixed with areas of disaggregation.

**Basin/Marsh Type**

Coastal Louisiana is divided into nine hydrologic basins and five vegetation zones (forested wetland, fresh, intermediate, brackish, and saline marsh) (Fig. 1). These basins contain landscapes of varying composition and configurations, and are subject to different processes impacting the development of those landscapes. It is therefore useful to examine landscape aggregation in each of these basins.

Across all basin/marsh type combinations, intermediate marsh in Breton Sound Basin was shown to have experienced the greatest reduction in AI over the time period, with a trend toward disaggregation of 0.92 %/year (Fig. 6c, Table 2). In reality, the trend in this area has not been linear however and experienced an extreme disturbance from Hurricane Katrina in 2005 and Hurricane Gustav in 2008. Wetland loss and the fragmentation associated with hurricanes Katrina, Rita, Gustav, and Ike has been well documented (Barras 2006, 2009). These events

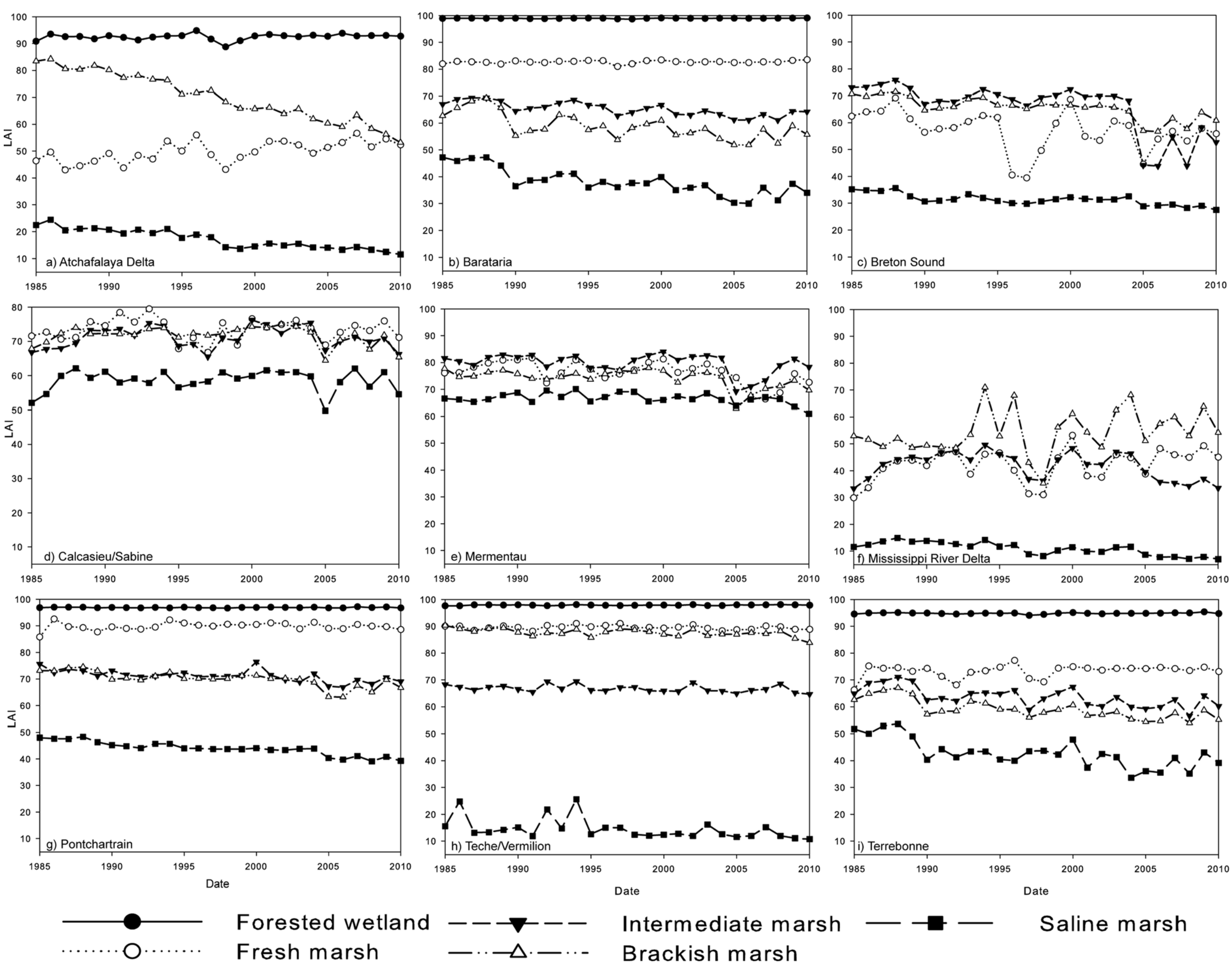


**Fig. 6** Average landscape aggregation index by basin and marsh type in coastal Louisiana (1985–2010) **a** Atchafalaya Delta, **b** Barataria, **c** Breton Sound, **d** Calcasieu-Sabine, **e** Mermentau, **f** Mississippi River Delta, **g** Terrebonne, **h** Teche-Vermilion, **i** Pontchartrain, basins

**Table 2** AI linear change statistics by basin and marsh type

| Basin | Forested Wetland | | | Fresh Marsh | | | Intermediate Marsh | | | Brackish Marsh | | | Saline Marsh | | |
|---|---|---|---|---|---|---|---|---|---|---|---|---|---|---|---|
| | Slope | $r^2$ | *P*-value | Slope | $r^2$ | *P*-value | Slope | $r^2$ | *P*-value | Slope | $r^2$ | *P*-value | Slope | $r^2$ | *P*-value |
| Atchafalaya Delta | 0.0335 | 0.05 | 0.268414* | 0.3302 | 0.42 | 0.000343 | Insufficient sample size | | | −1.1761 | 0.97 | 3.01E-19 | −0.4445 | 0.89 | 7.07E-13 |
| Barataria | 0.0034 | 0.07 | 0.186041* | 0.0169 | 0.05 | 0.249978* | −0.2605 | 0.61 | 0.000002 | −0.4387 | 0.49 | 0.000065 | −0.5385 | 0.69 | 1.77E-07 |
| Breton Sound | Insufficient sample size | | | −0.3594 | 0.14 | 0.061146* | −0.9248 | 0.53 | 0.000022 | −0.4259 | 0.64 | 0.000001 | −0.2208 | 0.63 | 0.000001 |
| Calcasieu- Sabine | | | | −0.0039 | 0.00 | 0.964068* | 0.0246 | 0.00 | 0.769944* | −0.0787 | 0.05 | 0.271569* | 0.0170 | 0.00 | 0.837363* |
| Mermentau | | | | −0.2905 | 0.28 | 0.005598 | −0.1868 | 0.15 | 0.050515* | −0.2497 | 0.31 | 0.003274 | −0.1007 | 0.15 | 0.051910* |
| Mississippi River Delta | | | | 0.2890 | 0.14 | 0.061525* | −0.2174 | 0.11 | 0.103641* | 0.3329 | 0.10 | 0.114063* | −0.2590 | 0.68 | 2.14E-07 |
| Pontchartrain | 0.0009 | 0.00 | 0.797584* | 0.0260 | 0.02 | 0.484848* | −0.1900 | 0.43 | 0.000296 | −0.2927 | 0.59 | 0.000004 | −0.3175 | 0.86 | 1.18E-11 |
| Teche-Vermilion | 0.0060 | 0.10 | 0.110787* | −0.0234 | 0.05 | 0.249438* | −0.0666 | 0.15 | 0.052039* | −0.1081 | 0.34 | 0.001638 | −0.2388 | 0.22 | 0.015419* |
| Terrebonne | 0.0059 | 0.03 | 0.376239* | 0.0918 | 0.09 | 0.145550* | −0.3276 | 0.46 | 0.000138 | −0.3703 | 0.60 | 0.000003 | −0.5217 | 0.54 | 0.000017 |

P-values denoted with an asterisks indicate trends which were not significant at the $P < 0.0001$ level

can scour and remove marsh, thereby disaggregating marsh, but they can also lead to temporary flooding which can affect landscape composition and configuration estimates. It is both these permanent and transient effects which explain the low LAI values in 2006 and 2008 in Breton Sound, particularly in fresh and intermediate marshes.

Saline marsh in Barataria and Terrebonne basins experienced the second and third most significant trend toward disaggregation with disaggregation rates of 0.54 %/year and 0.52 %/year respectively. Following these areas, brackish marsh in Barataria, Breton Sound, and Terrebonne basins experienced the next highest disaggregation rates at 0.44 %/year, 0.43 %/year, and 0.37 %/year (Table 2). All of these landscapes occur in a band of elevated wetland loss and fragmentation occurring in the Deltaic plain (Fig. 5).

While fresh marsh occupies only a small portion of Breton Sound Basin, it has shown the next highest rate of disaggregation over the time period, with a rate of 0.36 %/year. The only portion of this basin in which fresh marsh occurs is a region surrounding a freshwater diversion (Caernarvon), and as such, water level variability can affect remotely sensed estimates of composition and configuration. The low AI values observed during the 1996–1997 time period (Fig. 6c) and the imagery from which the AI was calculated during these years, correspond to a period of above average discharge from the diversion. This region has also been affected by recent hurricanes including Katrina and Gustav.

Basin/marsh type trends vary spatially as shown in Fig. 6 and Table 2, with trends which mimic those of land change rates in wetlands of those regions. Generally, the higher the land loss rate occurring in a wetland area, the higher the rate of disaggregation, as is to be expected. Both wetland loss and fragmentation have been shown to increase along an increasing salinity gradient, and both loss and fragmentation in the Deltaic Plain far exceeded that in the Chenier Plain.

Of interest are the few basin/marsh type regions which are experiencing a trend toward aggregation. The regions with the highest rate of aggregation correspond to actively prograding deltas including fresh marsh in Atchafalaya Delta and Mississippi River Delta basins (aggregating at rates of 0.33 % and 0.29 %/year respectively). These areas are some of the only regions in coastal Louisiana which receive significant supplies of mineral sediment, and as such, have been experiencing growth (WLD and AD), or at least stability and apparent aggregation (MRD). Of note however is the high variability in the AI in some of the marsh zones in these active deltas including the brackish marsh in MRD (Fig. 6f). High water level variability due to the riverine influence contributes to this variability, and should be considered when interpreting trends in these areas.

## Evaluating Restoration Project Effect on Spatial Configuration

The Coastal Wetlands Planning, Protection and Restoration Act (CWPPRA) program began in 1990 and its purpose is to identify, plan, and construct coastal restoration projects. CWPPRA has built over 100 restoration projects in coastal Louisiana since its inception, with another 50 funded for engineering and design (LA CWPPRA TF 2012). Examples of project types are hydrologic restoration, marsh creation, shoreline protection, marsh management, sediment and freshwater diversions, and vegetative planting.

In order to evaluate restoration effects on aggregation, the tool was used to calculate LAI for a selection of constructed CWPPRA restoration projects (Fig. 7). Both pre- and post-construction trends were analyzed and compared to land area change trends. The AI linear trends mimicked that of land area change trends for the projects.

Bayou LaBranche Wetland Creation (PO-17) is a marsh creation project located in St. Charles Parish and is bounded by U.S. Interstate 10 to the south and Lake Pontchartrain to the north. The project construction was completed in 1994. As a result of the introduction of the elevated marsh platform, both AI and land change trends changed from negative to positive (Fig. 8a and b). This implied the project area is not only maintaining its land area, but also its spatial configuration. Variability in land area, as well as AI, were attributed to water level fluctuations within the project caused by ponding within the center of the project area. Once water got in, it may have taken longer to drain, thus the range in values post-construction. The November 2000 data point was excluded for this reason.

Lake Chapeau Sediment Input and Hydrologic Restoration, Point Au Fer (TE-26), which consists of hydrologic restoration and marsh creation components, was completed in 1999 and is located on Point Au Fer Island, east of Atchafalaya Bay. The marsh creation (0.65 km$^2$) is a small component of the total project area (56 km$^2$), so the immediate increase in AI and land area acres was not evident (Fig. 8c and d). The 2005 data point was excluded because the image was taken post-hurricane, and the change was not persistent. Both land change and AI trends shifted from negative to positive. The subtle change suggests the hydrologic restoration component has aided in the reduction and reversal of the land change and AI rates.

To examine how restoration projects in the delta areas of coastal Louisiana compare, two sediment placement projects were evaluated. Sediment placement projects consist of placing sediments, usually sand, in areas near the borrow source. Often these projects are referred to as beneficial use projects because the sediment source is the result of scheduled dredging to maintain channels. Dustpan Maintenance Dredging Operation for Marsh Creation in the MS River Delta Demonstration (MR-10) is located in the Mississippi River Delta and was completed in 2002. Prior to construction, AI and land area change rates were minimal and variability in observed values could be attributed to water level variations in the deltaic environment (Fig. 8e and f). The January 2000 data point

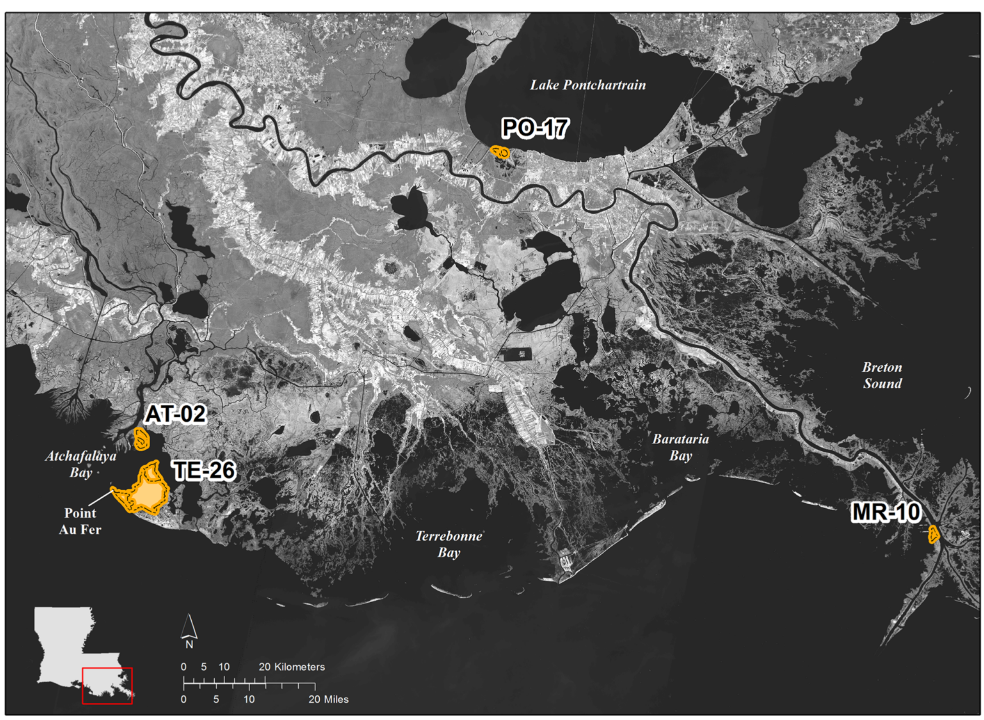


Fig. 7 Selected Coastal Wetlands Planning Protection and Restoration Act (CWPPRA) project locations

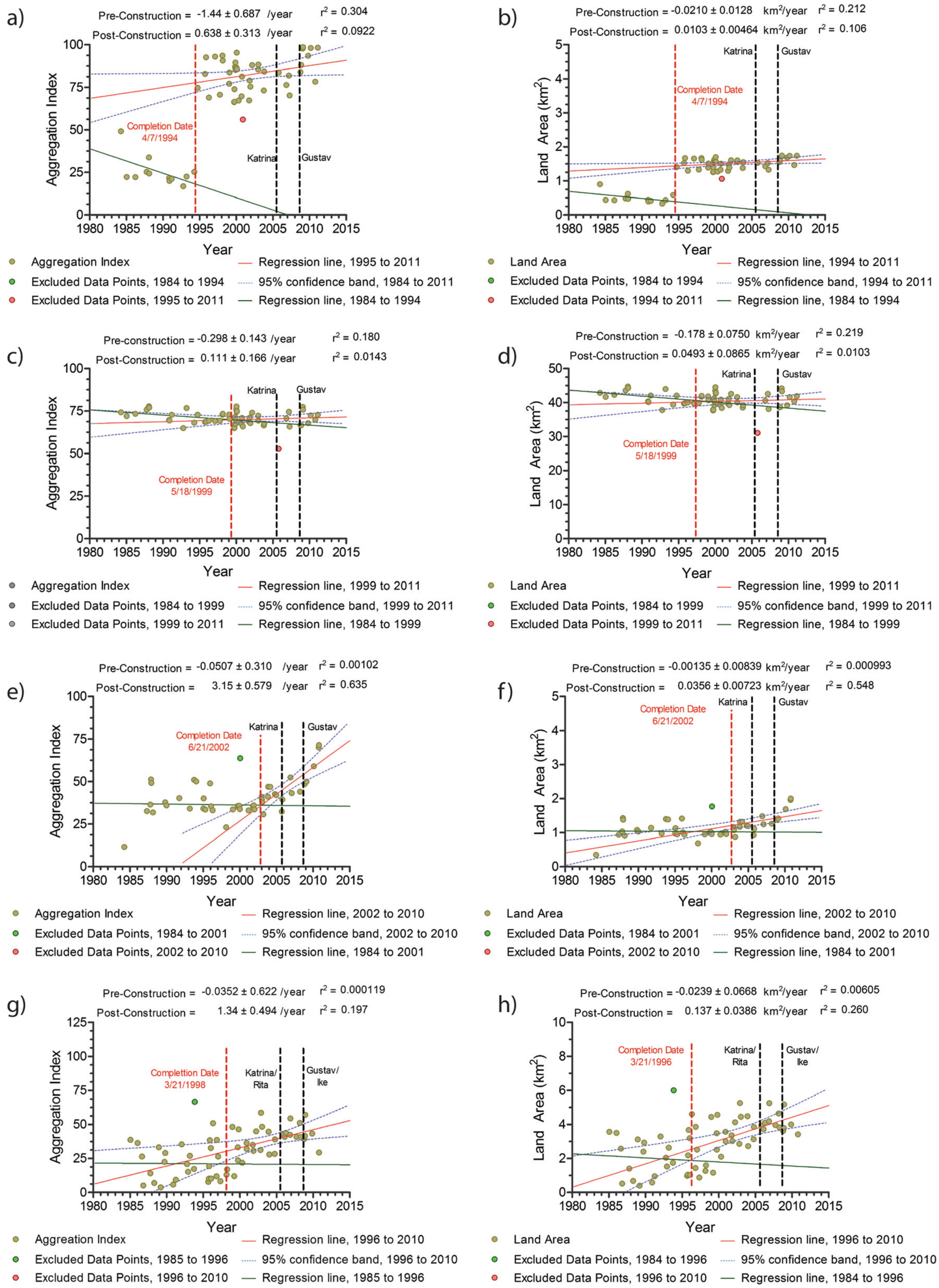


**Fig. 8** LAI and land area change trends for selected CWPPRA projects **a** PO-17 AI, **b** PO-17 land change, **c** TE-26 AI, **d** TE-26 land change, **e** MR-10 AI, **f** MR-10 land change, **g** AT-02 AI, and **h** AT-02 land change

was excluded from the analysis due to low water levels at the time of image acquisition that resulted in exposed mud flats and an over estimation of land during classification. After the dredged sediment was placed, variability decreased and both the AI and land change trends changed from slightly negative to positive. While the land change rate became positive, probably due to sediment placement, the positive change rate is similar to pre-construction. This suggests that the project area is not gaining land, but is maintaining land. Atchafalaya Sediment Delivery (AT-02) is located in the Atchafalaya Delta and construction was completed in 1998. Figure 8g and h show similar results to MR-10. Prior to construction, the land change rate was close to zero. Post-construction, the land change rate shifts to a more positive slope. This suggests that not only did the sediment placement aid the area by creating more aggregated land, but it is facilitating delta building. Due to water level influences within the deltaic project locations, AI and land area values were variable. The October 1993 data point was excluded from consideration due to low water levels at the time of the image acquisition, which resulted in mudflats that were recognized as land during image classification. In addition, low $r^2$ values can be attributed to the water level fluctuations and the moderate change rates.

### Link between Spatial Configuration and Susceptibility to Wetland Loss

While it is known that wetland loss contributes to fragmentation, and it is suspected that fragmentation contributes to wetland loss, few studies have actually tested that hypothesis at a landscape scale over a long period of record. To determine if such a relationship actually exists, we compared AI in a preceding time period to the rate of land change which would occur in subsequent time periods. For this assessment, AI was assessed on five dates: 1985, 1990, 1995, 2000, and 2005. A land change rate was then calculated for each 5 year period following that initial date. For example, AI in 1985 was compared to a land change rate calculated for the 1985–1990 time period. A land change rate is expressed as a percent per year of the remaining land at the beginning of each time period. The resulting land change rate and the AI from the preceding time period were then compared. The results are seen in Fig. 9 below.

These results suggest that spatial configuration of wetlands is not only a function of wetland loss, but also a contributor to the land change occurring in the region. While the causal mechanisms of wetland loss may lead to the initial fragmentation of wetlands, the fragmentation itself then contributes to increased exposure and vulnerability of wetland landscapes, thereby increasing the probability of furthered wetland loss. While the correlation coefficient observed (0.5562) is not particularly high, we know that there are many other causal mechanisms (such as subsidence, sea level rise, and availability of sediment) at play in the loss and fragmentation of wetlands. The existence of a significant ($P < 0.0001$) relationship is of interest as this is the first time that fragmentation has been shown to contribute to furthered wetland loss in coastal Louisiana.

### Impacts of Spatial Configuration

We have shown that fragmentation leads to increased susceptibility to wetland loss, a process which most would agree is a negative effect, the merit of other impacts of wetland fragmentation are more difficult to interpret. Haas et al. (2004) found that habitats containing more edge fostered an increased survival rate of brown shrimp by both providing more access to vegetation and reducing movement-related mortality. From a habitat perspective, a species may, at least initially, prefer landscape

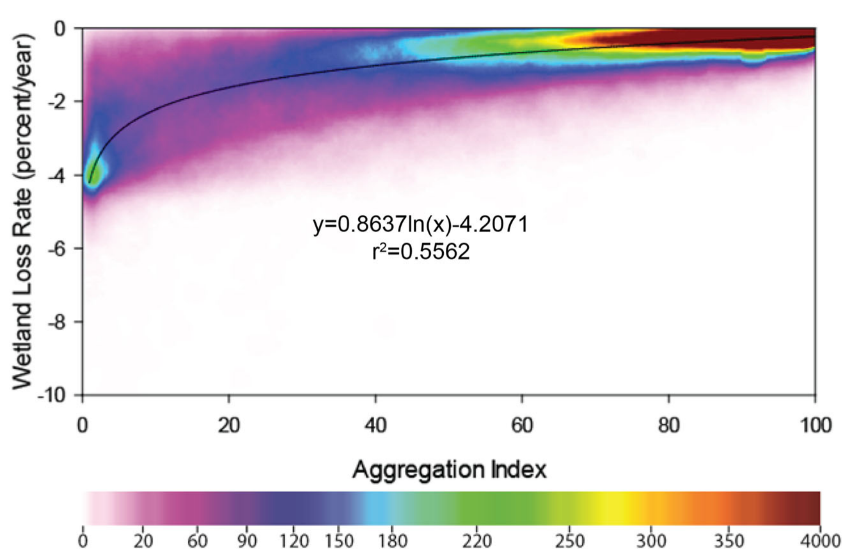


**Fig. 9** Relationship between aggregation index and land change rate in subsequent periods ($P < 0.0001$). Colors represent the point density of data points per unit of AI and per 0.1 %/year of land change rate

configurations which contain more edge, and consequently more habitat for species which utilize that edge. In this case however, edge can increase or decrease as a result of wetland loss depending upon landscape configuration. Edge will initially increase as a result of wetland loss and the resulting fragmentation of the landscape. This increase continues until a peak, at which continued wetland loss will lead to a decrease in edge, thus creating a curvilinear relationship between wetland loss and edge. This curve was first hypothesized by Browder et al. (1985).

Considerations of fishery habitat preferences aside, this study aims to assess the impact of wetland fragmentation on landscape stability, and assess the types of landscape configurations which promote that stability. Spatial integrity refers to the spatial extent, configuration and connectivity of wetland landscapes which support the persistence of those wetlands. From a spatial integrity standpoint, this study has shown that more contiguous, aggregated landscapes contribute to landscape stability.

## Conclusions

The distribution of wetlands in space is a key aspect determining a landscape's functionality and susceptibility to loss. Coastal Louisiana wetlands are being lost and as a result, the remaining landscape is becoming further disaggregated. In part, as a result of that disaggregation, more wetlands will be lost, creating a cycle that results in furthered loss of wetlands and the ecosystem services those wetlands provide.

If not restored, wetland loss and fragmentation will continue to result in dramatic changes in the pattern of the coastal Louisiana landscape. We argue that the restoration of not only spatial extent, but also configuration and connectivity of the wetlands is critical to the integrity and sustainability of the ecosystem. Restoration activities should pursue the creation of a landscape composed of patch configurations which exhibit persistence yet maintain moderate levels of hydrologic connectivity. Such a mosaic would promote functionality while balancing the risk of exposure, thus supporting both structural and functional integrity. In addition, the LAI tool could be used by project planners and decision makers to evaluate restoration projects and help determine locations where restoration dollars and resources can best be implemented.

Remote sensing technologies combined with landscape metrics have proven essential in studying these trends over time (O'Neill 1997, Yang and Liu 2005; Suir et al. 2013). Satellite imagery is useful due to the large number of historic images available over an extended period of record as well as wide spatial coverage. Numerous landscape metrics and types of imagery exist and future studies could look at other kinds of each in the hopes of better understanding coastal processes. Future improvements could be to better understand/estimate water levels at the time of satellite imagery capture. Having a better way to estimate the water levels will give us a greater understanding of anomalies which may be seen in the classified land/water imagery. This may be due to abnormally high water which can lead to marsh flooding or abnormally low water which may expose mud flats and make land appear more widespread than it is in actuality. If we could find a method to normalize for water levels it could improve our land/water datasets which in turn will improve our aggregation index output.

**Acknowledgments** This research was supported by the United States Geological Survey National Wetlands Research Center as well as the Coastwide Reference Monitoring System (CRMS).

**Compliance with Ethical Standards**

**Disclaimer** Any use of trade, firm, or product names is for descriptive purposes only and does not imply endorsement by the U.S. Government.

## References

Barras JA (2006) Land area change in coastal Louisiana after the 2005 hurricanes—a series of three maps: U.S. Geological Survey Open-File Report 2006–1274. (Also available at http://pubs.usgs.gov/of/2006/1274/)

Barras JA (2007) Land area changes in coastal Louisiana after Hurricanes Katrina and Rita. In: Farris GS, Smith GJ, Crane MP, Demas CR, Robbins LL, Lavoie DL (eds) Science and the storms—the USGS response to the hurricanes of 2005: U.S. Geological Survey Circular 1306, p. 97–112. (Also available at http://pubs.usgs.gov/circ/1306/)

Barras JA (2009) Land area change and overview of major hurricane impacts in coastal Louisiana, 2004–08: U.S. Geological Survey Scientific Investigations Map 3080, scale 1:250,000, 6 p. pamphlet

Browder JA, Bartley HA, Davis KS (1985) A probabilistic model of the relationship between marshland/water interface and marsh disintegration. Ecological Modelling 29:245–260

Bureau of Transportation Statistics (2013) Table 2–57: tonnage of top 50 U.S. Water Ports, Ranked by Total Tons. http://www.rita.dot.gov/bts/sites/rita.dot.gov.bts/files/publications/national_transportation_statistics/html/table_01_57.html. Accessed 09 June 2015

Couvillion BR, Barras JA, Steyer GD, Sleavin W, Fischer M, Beck H, Trahan N, Griffin B, Heckman D (2011) Land area change in coastal Louisiana from 1932 to 2010: U.S. Geological Survey Scientific Investigations Map 3164, scale 1:265,000, 12 p. pamphlet

DeMarco K, Mouton J, Pahl J (2012) Recommendations for anticipating sea-level rise impacts on Louisiana coastal resources during project planning and design. Coastal Protection and Restoration Authority of Louisiana, Baton Rouge. Technical report, 65p. URL: http://www.lacpra.org/assets/docs/LACES/LACEStech02_06_12.pdf. Accessed 1 May 2012

Forman RTT (1995) Land mosaics: the ecology of landscapes and regions. Cambridge University Press, Cambridge

Haas HL, Rose KA, Fry B, Minello TJ, Rozas LP (2004) Brown shrimp on the edge: linking habitat to survival using an individual-based simulation model. Ecological Applications 14(4):1232–1247

Harris LD (1988) The nature of cumulative impacts on biotic diversity of wetland vertebrates. Environmental Management 12:675–693

He SH, DeZonia BE, Mladenoff DJ (2000) An aggregation index (AI) to quantify spatial patterns of landscapes. Landscape Ecology 15:591–601

Jaeger JA (2000) Landscape division, splitting index, and effective mesh size: new measures of landscape fragmentation. Landscape Ecology 15:115–130

Kelly M, Tuxen KA, Stralberg D (2011) Mapping changes to vegetation pattern in a restoring wetland: finding pattern metrics that are consistent across spatial scale and time. Ecological Indicators 11:263–273

Kupfer JA (2012) Landscape ecology and biogeography: rethinking landscape metrics in a post-FRAGSTATS landscape. Progress in Physical Geography 36(3):400–420

Louisiana Coastal Wetlands Conservation and Restoration Task Force (LA CWPPRA TF) (2012) The 2012 evaluation report to the U.S. congress on the effectiveness of coastal wetlands planning, protection and restoration act projects. http://lacoast.gov/reports/rtc/RTC_2012_1-18-13.pdf

Louisiana Department of Natural Resources (LA DNR), Technology Assessment Division (2004) Louisiana energy facts annual 2003. http://dnr.louisiana.gov/assets/docs/energy/newsletters/energy_facts_annual/LEF_2003.pdf. Accessed 09 June 2015

McGarigal K (2002) Landscape pattern metrics. In: El-Shaarawi AH, Piegorsch WW (eds) Encyclopedia of environmetrics, vol 2. Wiley, Chichester, pp 1135–1142

National Oceanic and Atmospheric Administration (NOAA) (2010) Annual commercial landing statistics. http://www.st.nmfs.noaa.gov/st1/commercial/landings/annual_landings.html. Accessed 09 June 2015

Neel MC, McGarigal K, Cushman SA (2004) Behavior of class-level landscape metrics across gradients of class aggregation and area. Landscape Ecology 19:435–455

O'Neill RV, Hunsaker CT, Jones KB, Riitters KH, Wickham JD, Schwartz PM, Goodman IA, Jackson BL, Baillargeon WS (1997) Monitoring environmental quality at the landscape scale. Bioscience 47(8):513–519

Peyronnin N, Green M, Richards CP, Owens A, Reed D, Chamberlain J, Groves DG, Rhinehart WK, Belhadjali K (2013) Louisiana's 2012 coastal master plan: overview of a science-based and publicly informed decision-making process. Journal of Coastal Research 67:1–15

Sasser CE, Visser JM, Mouton E, Linscombe J, Hartley SB (2014) Vegetation types in coastal Louisiana in 2013: U.S. Geological Survey Scientific Investigations Map 3290, 1 sheet, scale 1:550, 000. doi:10.3133/sim3290

Saura S (2004) Effects of remote sensor spatial resolution and data aggregation on selected fragmentation indices. Landscape Ecology 19: 197–209

Suir GM, Evers DE, Steyer GD, Sasser CE (2013) Development of a reproducible method for determining quantity of water and its configuration in the marsh landscape. Journal of Coastal Research 63: 110–117

Tischendorf L (2001) Can landscape indices predict ecological processes consistently? Landscape Ecology 16:235–254

Turner RE, Rao YS (1990) Relationships between wetland fragmentation and recent hydrologic changes in a deltaic coast. Estuaries 13(3): 272–281

Xu H (2006) Modification of normalised difference water index (NDWI) to enhance open water features in remotely sensed imagery. International Journal of Remote Sensing 27(14):3025–3033

Yang X, Liu Z (2005) Quantifying landscape pattern and its change in an estuarine watershed using satellite imagery and landscape metrics. International Journal of Remote Sensing 26(23):5297–5323